Optics Letters

Buckling-induced wavy optical fiber attenuator

Yu-Han Wang,[1] Zhu-Long Xu,[1] Yong Wang,[1] Hanqing Jiang,[2] and Kuo-Chih Chuang[1,*]

[1]Key Laboratory of Soft Machines and Smart Devices of Zhejiang Province, School of Aeronautics and Astronautics, Institute of Applied Mechanics, Zhejiang University, Hangzhou, 310027, China
[2]School of Engineering, Westlake University, Hangzhou, 310024, China
* Corresponding author: chuangkc@zju.edu.cn

Received 16 June 2022; revised 20 August 2022; accepted 22 August 2022; posted 23 August 2022; published 15 September 2022

An optical attenuator is an optical device that can modulate the power level of an optical signal. Based on the macro-bending loss of optical fibers, we present a wavy fiber attenuator where the attenuation level can be controlled by a mechanical-induced buckling of the fiber. By bonding a fiber to a prestretched substrate and then releasing the prestrain, the fiber flexes into a sinusoidal wavy curve due to the constraints of the substrate. The level of the light attenuation can simply be controlled by stretching the substrate. The maximum attenuation of the proposed wavy optical fiber attenuator is −87.3 dB.

https://doi.org/10.1364/OL.468102

Optical attenuators are widely used optical devices in the laboratory or communication networks to control (mainly reduce) the power level of optical signals [1–5]. In the application of optics-based sensing, without a proper power attenuation, the monitored signal might even be saturated and fail to provide true sensing information. Until now, several advanced attenuation mechanisms, including arranging obstructing elements with micromechanics [6–10], doping materials [11], or microelectron-mechanical system (MEMS) [12–14], to name a few, have been employed on fabricating optical attenuators. Although most recently developed mechanisms are compact and reliable, their fabrication might be challenging and their cost might be high.

It is well known that bending a fiber provides a simple mechanical route for achieving light attenuation. Micro-bending loss of the optical fiber [15,16], realized by squeezing the fiber, is a fundamental and common mechanism for attenuating the guided light. Interestingly, macro-bending is seldom used to realize optical fiber attenuation despite being simpler and more straightforward. This is mainly because of the difficulty to achieve a controllable curvature and accordingly a controllable attenuation level [17,18]. In mechanics, deterministic buckling structures have recently been applied in various fields, ranging from stretchable electronic interconnects to biocompatible topographic matrices for cell alignment [19,20]. To date, developed mechanical instability-based deterministic structures are usually realized by combining two mismatched materials such as a stiff two-dimensional stripe or film on a compliant substrate [21]. One interesting question to ask is whether the deterministic wave-like structures with mechanical instability can be harvested to turn a free-bending optical fiber into a curvature-controllable one and in turn control the level of attenuation.

In this Letter, we realize a tunable optical attenuator based on the buckling of a fiber. We fabricate a wavy fiber attenuator where the wavy profile is obtained from the mechanical contraction of a mismatched substrate. Since light is leaked when the fiber is bent, we will show that a controllable attenuation of the optical power can be achieved due to the deterministic and controllable curvature.

We first introduce the fabrication process of the wavy fiber attenuator, formed by gluing a section of an optical fiber on a mismatched soft substrate. As shown in Figs. 1(a)–1(c), an elastomer substrate is prestretched and then an optical fiber is firmly bonded to the substrate along the middle line of the upper surface. By releasing the prestrain, the substrate is compressed and a wavy profile can be obtained due to the buckling of the fiber. An elastomer substrate (Ecoflex00–30, Smooth-on Inc.) with dimensions of 150 mm × 50 mm × 2 mm is used for the fabrication of the attenuator. With a 10-mm clamping at the two ends, the initial length of the substrate is 130 mm. A 30% prestrain is considered and an adhesive glue (5562 instant adhesive, Shenzhen Kaibingtuan Plastic Industry Co., Ltd.) is used for bonding the fiber. The oblique view and the lateral view of the fabricated wavy fiber attenuator are showed in Figs. 1(d) and 1(e). Note that the quality of the fabrication of the proposed wavy attenuator depends on the prestrain of the substrate and the uniformness of the substrate and glue. When these factors are well controlled, the fabrication repeatability can be ensured. Figure 1(f) illustrates the variation of the wavelength and amplitude of the wavy profile and the corresponding attenuated light with respect to the strain of the substrate. In general, a larger strain of the substrate will lead to a shorter wavelength of the morphology obtained by buckling and less attenuated light. For a fabricated wavy fiber attenuator, the curvature of the fiber decreases when it is stretched by an external force until the fiber is straightened.

Although the shape of an optical fiber is round, it is thin and thus we can provide an approximate waveform of the wrinkled optical fiber where the description of the waveform borrows the finite deformation mechanics of a buckled thin film of thickness h on a compliant support [22–24]. For a fiber of a diameter D and elastic modulus E_f, and a substrate of elastic modulus E_s and prestrain ε_{pre}, the waveform of the buckling profile of the

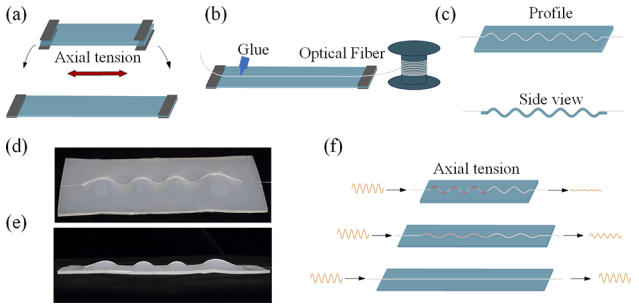

Fig. 1. (a)–(c) Fabrication process. (d) Oblique view of the sample. (e) Lateral view of the sample. (f) Illustration of the stretching process.

optical fiber is expressed as

$$w = A\cos\left(\frac{2\pi}{\lambda}x\right), \tag{1}$$

where the wavelength is

$$\lambda = \frac{\lambda_0}{(1+\varepsilon_{pre})(1+\xi)^{1/3}}, \tag{2}$$

where

$$\lambda_0 = 2\pi D\left(\frac{\overline{E_f}}{3\overline{E_s}}\right)^{\frac{1}{3}} \tag{3}$$

and

$$\xi = 5\varepsilon_{pre}(1+\varepsilon_{pre})/32. \tag{4}$$

The amplitude of the wavy fiber is

$$A = \frac{A_0}{\sqrt{1+\varepsilon_{pre}}(1+\xi)^{1/3}}, \tag{5}$$

where

$$A_0 = D\sqrt{\frac{|\varepsilon_{pre}|}{\varepsilon_c} - 1}, \tag{6}$$

where ε_c is the critical buckling strain as

$$\varepsilon_c = \frac{1}{4}\left(\frac{3\overline{E_s}}{\overline{E_f}}\right)^{2/3}. \tag{7}$$

When the buckled wavy fiber is subjected to an applied strain $\varepsilon_{applied}$, the wavelength and amplitude of the wavy fiber profile respectively become

$$\lambda = \frac{\lambda_0(1+\varepsilon_{applied})}{(1+\varepsilon_{pre})(1+\varepsilon_{applied}+\zeta)^{1/3}} \tag{8}$$

and

$$A = D\frac{\sqrt{(\varepsilon_{pre}-\varepsilon_{applied})/\varepsilon_c - 1}}{\sqrt{1+\varepsilon_{pre}}(1+\varepsilon_{applied}+\zeta)^{1/3}}, \tag{9}$$

where

$$\zeta = 5(\varepsilon_{pre}-\varepsilon_{applied})(1+\varepsilon_{pre})/32. \tag{10}$$

According to the buckling model, we get the relation between the wavelength and amplitude with respect to the prestrain of the substrate, as shown in Fig. 2(a). In calculating the buckling behavior, the following elastic constants are used: the modulus and the Poisson ratio of the optical fiber are respectively $E_f = 24$ GPa and $v_f = 0.33$, while those of the substrate are

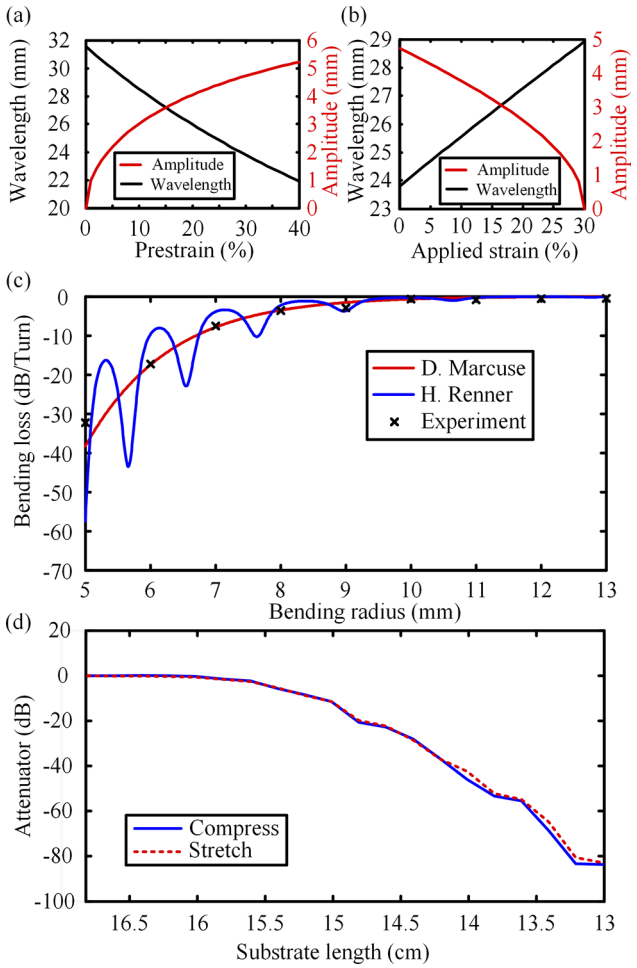

Fig. 2. (a) Wavelength and amplitude of sinusoidal morphology of the fiber in the range of 0–40% prestrain. (b) Wavelength and amplitude of the sinusoidal morphology of the fiber change with the applied strain when the prestrain is 30%. (c) Relation between light loss and fiber curvature radius. (d) Experimental result of the attenuation behavior of the wavy attenuator.

$E_s = 68$ kPa and $v_s = 0.33$, respectively. The relation between the wavelength and amplitude with respect to the applied strain of the substrate when the buckling fiber is subjected to an applied strain $\varepsilon_{applied}$ with a 30% prestrain is showed in Fig. 2(b).

After calculating the buckling behavior of the wavy profile, we show the attenuation characteristics of the optical fiber (Corning SMF-28) used in this work, according to the theory of optical macro-bending loss. For a bending fiber of length L, the pure bending loss can be calculated by $10\log_{10}(\exp(\gamma L)) = 4.343\gamma L$, where γ is the bending loss factor. There are two common models for calculating the macro-bending loss factor of the single-mode fiber, one from D. Marcuse and the other from H. Renner. D. Marcuse assumed that the fiber has an infinite cladding, and the corresponding bending loss factor is [25,26]

$$\gamma = \left(\frac{\pi}{4aR_c}\right)^{1/2}\left[\frac{U}{VK_1(W)}\right]^2\frac{1}{W^{3/2}}\exp\left[-\frac{2W^3}{3k_0^2a^3n_1^2}R_c\right], \tag{11}$$

where a is the core radius of the fiber, R_c is the bending radius, n_1 is the refractive index of the core, β is the propagation constant of the fundamental mode of a straight optical fiber, λ is the light

wavelength, $k_0 = 2\pi/\lambda$ is the wavenumber, $V = 2\pi a\frac{\sqrt{n_1^2-n_2^2}}{\lambda}$ is the normalized frequency, $U = a\sqrt{n_1^2k_0^2 - \beta^2}$, and $W = a\sqrt{\beta^2 - n_2^2k_0^2}$. Unlike the infinite-cladding model, H. Renner assumed that there is an infinite coating layer outside the fiber cladding and improved the calculation formula for the bending loss factor as [27]

$$\gamma_{Renner} = \gamma\frac{2\sqrt{Z_2Z_3}}{(Z_3+Z_2)-(Z_3-Z_2)\cos(2\theta_0)}, \tag{12}$$

where

$$Z_q = -(2k^2n_q^2/R_c)^{2/3}X_q(d,0),\ q = 2,3, \tag{13}$$

$$X_q(d,0) = (\frac{R_c}{2k^2n_q^2})^{3/2}[\beta^2 - k^2n_q^2(1+\frac{d}{R})], \tag{14}$$

and

$$\theta_0 = 2(-X_2(d,0))^{3/2}/3 + \pi/4, \tag{15}$$

where d is the diameter of the cladding, n_2 is the refractive index of the cladding, and n_3 is the refractive index of the coating.

The experimental and theoretical results of the bending loss with respect to the bending curvature of the SMF-28 are shown in Fig. 2(c). Slight oscillation can be found in the experimental result when the bending radius is small, which agrees with the prediction by the model of H. Renner. It should be noted that, by using a pointwise integration through the buckling fiber, the buckling model and the bending loss mode can be combined to obtain the complicated bending loss behavior. The attenuation behavior of the wavy attenuator using a 1550-nm distributed feedback (DFB) laser, where the two edges of the attenuator are connected to a single-axis tensile instrument, is shown in Fig. 2(d). We can see that the power of the wavy attenuator significantly decreases as the substrate is compressed. A rather linear region can be obtained during the compression or elongation of the wavy attenuator. The maximum attenuation is −87.3dB. However, the wavy attenuator is not sensitive when the applied strain is less than 10%. From Fig. 2(d), we can also see that the repeatability of the wavy attenuator is good by the fact that the curves of compression and elongation almost overlap. Time stability of the proposed wavy fiber attenuator is tested for 30 min when a 10% prestrain is applied with only a small total deviation of 0.57 dB (i.e., with a low time sensitivity of −0.019 dB/min). The effect of temperature on the sensor is also tested, where an average attenuation of −28.34 dB is measured in the temperature range of 6–65°C (i.e., with a low temperature sensitivity of −0.027 dB/°C). Finally, the durability of the proposed wavy attenuator in terms of applied strain was tested using the single-axis tensile instrument. The attenuation profile was maintained even after 1000 repeating cycles of loading and relaxing. Details of the testing of the time and temperature stability as well as the durability of the wavy attenuator during cyclic loading are provided in Supplement 1.

After theoretically studying the relation between the deformation of the substrate and curvature of optical fiber and experimentally demonstrating the attenuation behavior of the wavy attenuator, we demonstrate the capability of the wavy attenuator on modulating the power of optical devices, where here a fiber Bragg grating (FBG) is considered. The experimental setup is shown in Fig. 3(a). A broadband source transmits light to the wavy fiber attenuator [as shown in Figs. 1(d) and 1(e)], where a single-axis tensile instrument is used to control the curvature of the wavy attenuator. The light continues to direct to a fiber Bragg grating (FBG) by an optical circulator.

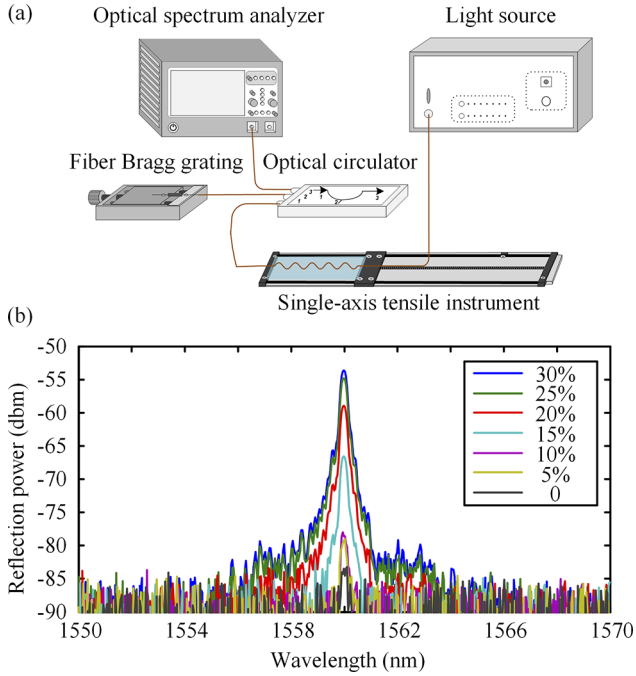

Fig. 3. (a) Experimental arrangement of the wavy attenuator in the application of the fiber Bragg grating. (b) Experimental result of the modulated reflected Bragg wavelength of the FBG.

Then, the reflected light from the FBG is transmitted back to the optical circulator and directed to an optical spectrum analyzer (OSA), with a minimum resolution of 0.02 nm.

The experimental result of modulating the reflected Bragg wavelength of the FBG is shown in Fig. 3(b), where a set of spectrometer data was recorded for every 5% of stretching. We can see that the trend of the peak of the Bragg wavelength decreases monotonically in power as the substrate is compressed. It is observed that the proposed wavy fiber attenuator can thoroughly turn on and turn off the reflected spectrum of the FBG. However, the profile and the central wavelength of the spectra of the FBG

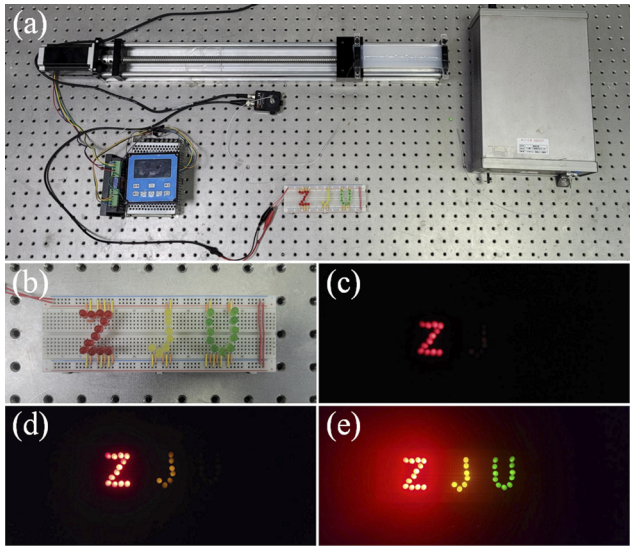

Fig. 4. (a) Experimental arrangement of the wavy attenuator in the application of voltage control. (b) Effect visualized by lighting "ZJU" luminous diodes.

are not affected by the stretching of the substrate, which is a desired characteristic as an optical attenuator.

Finally, we use light-emitting diodes (LEDs) to visualize the attenuation behavior of the proposed wavy attenuator. Figure 4(a) shows the arrangement of the experiment. The light signal, connected to the proposed wavy attenuator, is converted to an electrical signal by a photodiode to power the LEDs. The LEDs are arranged as the letters of "ZJU", where "Z" is formed by red LEDs, "J" by yellow ones, and "U" by blue ones. The operating voltage for the red LEDs is 1.7–2.4 V, for the yellow LEDs is 1.8–2.6 V, and for the green LEDs is 1.9–2.7 V. Due to different operating voltage, from Figs. 4(b)–4(e), we can see the LEDs can be lit up with different orders, indicating that the proposed wavy attenuator can be applied in the design of photoelectric circuits.

In conclusion, we introduce a wavy fiber attenuator based on the mechanics-induced buckling of optical fibers, which can cover the range from allowing light to pass through completely to forbidding light completely. The morphology of the optical fiber after buckling is analyzed theoretically and the effect of the proposed wavy attenuator is verified experimentally. In addition to simple fabrication, the switch and control of optical power can be realized by simple mechanical stretching and shrinking.

Funding. National Natural Science Foundation of China (11872328, 11972318, 12132013); Joint Fund of Science and Technology Department of Liaoning Province and State Key Laboratory of Robotics China (2020-KF-22-09).

Disclosures. The authors declare no conflicts of interest.

Data availability. Data underlying the results presented in this paper are not publicly available at this time but may be obtained from the authors upon reasonable request.

Supplemental document. See Supplement 1 for supporting content.

REFERENCES

1. Z. Tian, S. S. Yam, and H.-P. Loock, IEEE Photonics Technol. Lett. **20**, 1387 (2008).
2. Z. Chen, K. Chiang, K. Lee, and K. Lor, Microwave. Opt. Technol. Lett. **26**, 1 (2000).
3. D.-H. Lee, K.-H. Kwon, J.-W. Song, and J.-H. Park, J. Opt. Soc. Korea **8**, 83 (2004).
4. V. K. Hsiao, Z. Li, Z. Chen, P.-C. Peng, and J. Tang, Opt. Express **17**, 19988 (2009).
5. H. Ahmad and A. Al-Alimi, Appl. Opt. **59**, 1876 (2020).
6. C. Marxer, P. Griss, and N. F. de Rooij, IEEE Photonics Technol. Lett. **11**, 233 (1999).
7. H. Lotem, A. Eyal, and R. Shuker, Opt. Lett. **16**, 690 (1991).
8. J. E. Ford and J. A. Walker, IEEE Photonics Technol. Lett. **10**, 1440 (1998).
9. C. Rembe, H. Aschemann, S. aus der Wiesche, E. Hofer, H. Debeda, J. Mohr, and U. Wallrabe, in *2000 IEEE International Reliability Physics Symposium Proceedings. 38th Annual (Cat. No.00CH37059)* (IEEE, 2000).
10. H. Ren and S.-T. Wu, Opt. Lett. **35**, 3826 (2010).
11. Y. Morishita, E. Matsuyama, K. Nouchi, H. Noro, and K. Tanaka, Opt. Lett. **26**, 783 (2001).
12. A. Lagosh, B. Guldimann, G. Huszka, H. Sattari, B. Ahlers, G. Kerr, M. Melozzi, P. Rahnama, T. Nishizawa, and N. Quack, in *2021 IEEE 34th International Conference on Micro Electro Mechanical Systems (MEMS)* (IEEE, 2021).
13. N. A. Riza and S. Sumriddetchkajorn, Opt. Lett. **24**, 282 (1999).
14. I. Kumar and P. K. Pattnaik, in *2019 3rd International Conference on Computing Methodologies and Communication (ICCMC)* (IEEE, 2019).
15. D.-W. Huang, W.-F. Liu, and C. Yang, IEEE Photonics Technol. Lett. **12**, 1153 (2000).
16. S. Ward, R. Allahverdi, and A. Mafi, Opt. Commun. **507**, 127743 (2022).
17. Q. Wang, G. Rajan, G. Farrell, P. Wang, Y. Semenova, and T. Freir, Meas. Sci. Technol. **18**, 3082 (2007).
18. X. Peng, Y. Cha, H. Zhang, Y. Li, and J. Ye, Opt. Eng. **56**, 066102 (2017).
19. T. Q. Trung and N. E. Lee, Adv. Mater. **29**, 1603167 (2017).
20. M. Gonzalez, F. Axisa, M. V. Bulcke, D. Brosteaux, B. Vandevelde, and J. Vanfleteren, Microelectron. Reliab. **48**, 825 (2008).
21. N. Bowden, S. Brittain, A. G. Evans, J. W. Hutchinson, and G. M. Whitesides, Nature **393**, 146 (1998).
22. H. Jiang, D.-Y. Khang, J. Song, Y. Sun, Y. Huang, and J. A. Rogers, Proc. Natl. Acad. Sci. U. S. A. **104**, 15607 (2007).
23. Z. Huang, W. Hong, and Z. Suo, J. Mech. Phys. Solids **53**, 2101 (2005).
24. H. Jiang, D.-Y. Khang, H. Fei, H. Kim, Y. Huang, J. Xiao, and J. A. Rogers, J. Mech. Phys. Solids **56**, 2585 (2008).
25. D. Marcuse, J. Opt. Soc. Am. **66**, 216 (1976).
26. D. Marcuse, J. Opt. Soc. Am. **66**, 311 (1976).
27. H. Renner, J. Lightwave Technol. **10**, 544 (1992).